BIOCHEMISTRY
including biophysical chemistry & molecular biology

Article

pubs.acs.org/biochemistry

The RNA Aptamer Inhibiting Human Vesicular Endothelial Growth Factor Receptor 1 without Affecting Cytokine Binding

Shoji P. Ohuchi,[†] Masabumi Shibuya,[‡] and Yoshikazu Nakamura*[,†]

[†]Institute of Medical Science, University of Tokyo, 4-6-1 Shirokanedai, Minato-ku, Tokyo 108-8639, Japan

[‡]Gakubunkan Institute of Physiology and Medicine, Jobu University, Takasaki 370-1393 Japan

Supporting Information

ABSTRACT: Angiogenesis, a process of new blood vessel formation, is crucial not only for many physiological events but also for a number of diseases. The signaling pathways through members of the vesicular endothelial growth factor (VEGF) family play fundamental roles in angiogenesis. In this study, we identified inhibitory RNA aptamers against human Flt-1, a receptor of VEGF. One of the isolates, aptamer #38, showed a 50% inhibitory concentration (IC_{50}) of 23 nM in the cell-based autophosphorylation assay, and the IC_{50} value was decreased to 6.3 nM upon removal of 32 dispensable nucleotides from parental #38 with a length of 72 nucleotides. Interestingly, the surface plasmon resonance-based or affinity resin-based binding study revealed that #38 and its shortened derivative, #38Jr, do not interfere with binding of VEGF or heparin, a functional cofactor, to Flt-1. Importantly, aptamer #38 does not affect the decoy activity of soluble Flt-1. These findings suggest that #38 prevents the conformational activation of Flt-1 associated with VEGF. Therefore, aptamer #38 might provide us with a unique tool for blocking the VEGF signaling specific to Flt-1, unlike most other known VEGF signaling blockers such as VEGF inhibitors, anti-Flt-1 antibodies, and decoy soluble receptors.

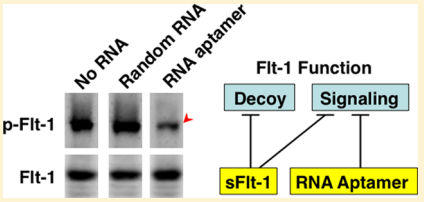

Angiogenesis, a complex process of new blood vessel formation, involves a number of different growth factors. It is essential not only for many physiological events but also for a number of diseases, including tumor progression, psoriasis, rheumatoid arthritis, and diabetic retinopathy.[1−3] The signaling pathways through members of the vesicular endothelial growth factor (VEGF) family play fundamental roles in angiogenesis. VEGF family cytokines function mainly through binding to the three homologous receptor tyrosine kinases, VEGF receptors (VEGFR1−3). Although VEGFR2 (also known as KDR) is thought to be a central receptor for the pathways,[1−3] we recently became aware of the physiological roles of the other two receptors and their relationships to diseases.

VEGFR1, also named Flt-1, is essential for the vascular system organization,[4] but expression of an Flt-1 mutant defective only in the tyrosine kinase activity is sufficient for the normal embryogenesis of mice.[5] Thus, it has been suggested that Flt-1 acts as a nonsignaling reservoir or a decoy receptor.[6] However, the physiological significance of Flt-1-dependent signaling has been demonstrated recently. Not only endothelial cells but also pluripotent stem cells express Flt-1 on their surface, and the Flt-1-specific cytokine, placental growth factor (PlGF), can reconstitute hematopoiesis by recruiting the stem cells from the bone marrow.[7] In addition, selective activation of Flt-1 induces proliferation of hepatocytes rather than endothelial cells.[8] Although PlGF is not required for embryogenic angiogenesis,[9] its knockout displayed attenuated responses to VEGF in pathological angiogenesis in mice.[10] Furthermore, PlGF is necessary for angiogenic events in adult tissues during ischemia, inflammation, wound healing, and cancer.[9] Thus, PlGF and Flt-1 might be attractive targets for the treatment of diseases involving inflammation and angiogenesis.[11]

Until now, several Flt-1 antagonists have been studied as drug leads. For example, antibodies against Flt-1 suppressed tumorigenic neovascularization, ischemic retina, and inflammatory joint destruction in autoimmune arthritis.[12] Hammerhead ribozyme-mediated knockdown of Flt-1 resulted in dose-dependent antimetastatic activity in the xenograft model of human colorectal cancer and mouse tumor models.[13−15] The short interfering RNA-mediated knockdown showed the suppression of laser injury-induced choroidal neovascularization in mice, though its exact mechanism is unclear.[16,17]

In this study, we aimed to isolate inhibitory RNA aptamers against human Flt-1 (hFlt-1) as the alternative drug lead. Aptamers are short single-stranded nucleic acid molecules that are selected in vitro from a large random sequence library based on their high affinity for a target molecule by a process known as SELEX (systematic evolution of ligands by exponential enrichment).[18−21] Similar to antibodies, aptamers show a high affinity and specificity against a target, as well as additional advantages, including their small size, easiness of chemical production, and antidote design.[21] One of the anti-Flt-1 aptamers selected in this study exhibits a unique inhibitory feature.

Received: December 17, 2012
Revised: February 15, 2013
Published: February 27, 2013

dx.doi.org/10.1021/bi301669p | *Biochemistry* 2013, 52, 2274−2279

MATERIALS AND METHODS

SELEX. RNAs with 2′-fluoropyrimidine modifications were prepared as previously described.[22] For the preparation of an initial DNA pool, a synthetic DNA was employed, 5′-TAATACGACT CACTATAGGG CTGAAGGATG CCA-N40-CCGAGTCGTG CCATCT-3′ [T7 promoter sequence underlined, and N40 represents 40 nucleotides (nt) of random sequence]. All synthetic DNAs were purchased from Operon Biotechnologies. SELEX was performed against recombinant extracellular domains of hFlt-1 fused to the C-terminal hexahistidine-tagged Fc region of human immunoglobulin G (IgG) (R&D Systems). Before the selection process, the purified RNAs were folded by being denatured at 94 °C for 3 min and then cooled to 4 °C and incubated in buffer A [20 mM Tris-HCl (pH 7.6), 150 mM NaCl, 1.5 mM $CaCl_2$, 0.5 mM $MgCl_2$, and 0.05% Tween 20] for 10 min at 37 °C. To reduce undesired, nonspecific adsorption of RNAs to resins, 2 mg/mL tRNA (Sigma-Aldrich) and 1 mg/mL bovine serum albumin (Sigma-Aldrich) were added to the folded RNAs.

Three types of resins, HisLink Protein Purification Resin (Promega), rProtein A Sepharose Fast Flow (GE healthcare), and anti-IgG aptamer-immobilized resin,[23] were alternatively utilized for the affinity capture of recombinant hFlt-1. Except for the first round, negative selection was performed before positive selection. For negative selection, the folded RNAs were transferred to 3 μL of HisLink Resin without protein immobilization, human IgG (Sigma-Aldrich)-immobilized Protein A, or anti-IgG aptamer resin followed by incubation for 10 min at room temperature. Then, the supernatant containing unbound RNAs was collected and subjected to positive selection. For positive selection, the RNAs were transferred to 3 μL of the indicated resin with the recombinant hFlt-1 immobilization, followed by incubation for 30 min at room temperature. After the samples had been washed for the indicated times with buffer A, tightly bound RNAs were eluted from the resin via addition of EDTA-containing buffer [20 mM Tris-HCl (pH 7.6) and 2 mM EDTA][24] and phenol/chloroform extraction. The recovered RNAs were subjected to reverse transcription, polymerase chain reaction, and in vitro transcription to regenerate an enriched RNA pool as previously described.[22] After five to nine rounds of SELEX, variants in the pool DNAs were cloned into a TA cloning vector (pGEM-T Easy, Promega). Detailed conditions for positive selection in each round are listed in Table 1.

Surface Plasmon Resonance (SPR) Assay. SPR analysis was performed as previously described[22] with minor modifications. Buffer A was employed as running buffer, and the data were obtained by subtracting the signals for a flow cell via immobilization of the initial pool RNA. Recombinant extracellular domains of human KDR were purchased from R&D Systems.

Autophosphorylation Assay. VEGF-stimulated autophosphorylation of Flt-1 or KDR was analyzed with 3T3-FLT-1 or 3T3-KDR cells, respectively.[25,26] The cell culture, VEGF stimulation, and Western blotting were essentially as described previously.[25,26] Detection of phosphorylated hFlt-1 was performed by using affinity-purified rabbit anti-phospho-Flt-1 (Y1213) (R&D Systems) and HRP-linked anti-rabbit IgG (GE healthcare) antibodies as the primary and secondary antibodies, respectively. Before the VEGF stimulation, $^1/_{10}$ volumes of the 10-fold indicated concentrations of the folded RNAs were added to the culture medium, followed by incubation at 37 °C for 5 min. Recombinant human $VEGF_{165}$ was purchased from R&D Systems.

Quantitative analysis of Flt-1 autophosphorylation was performed by the sandwich enzyme-linked immunosorbent assay (ELISA) using Duo Set Human Phospho-VEGF R1/Flt-1 (R&D Systems). The cell culture, VEGF stimulation, and sample preparation were as described above. The sandwich ELISA was performed according to the supplier's protocol.

Pull-Down Assay. The Flt-1 pull-down assay was performed by using Heparin Sepharose 6 Fast Flow (GE healthcare). The indicated concentrations of the RNAs were folded into 100 μL of buffer A as described above, mixed with recombinant hFlt-1 (final concentration of 10 nM), and incubated at 37 °C for 10 min. The mixture was added to 3 μL of the heparin resin and incubated at room temperature for 30 min. The resin was washed once with 100 μL of buffer A, and recombinant hFlt-1 recovered with the resin was subjected to 8% sodium dodecyl sulfate−polyacrylamide gel electrophoresis. Western blotting was performed with anti-Flt-1 (sc316, Santa Cruz Biotechnology) and HRP-linked anti-rabbit IgG (GE healthcare) antibodies as the primary and secondary antibodies, respectively, followed by the imaging analysis as previously described.[22]

Table 1. Conditions for Positive Selection against hFlt-1

round	[recombinant hFlt-1] (nM)	resin	no. of washings
1	250	anti-IgG aptamer	4
2	250	Protein A	6
3	125	nickel	6
4	125	Protein A	8
5	62.5	anti-IgG aptamer	8
6	62.5	nickel	10
7	31.3	Protein A	10
8	31.3	nickel	10
9	15.6	anti-IgG aptamer	10

RESULTS

Isolation of Inhibitory Aptamers against Human Flt-1. We isolated RNA aptamers against hFlt-1 by the SELEX procedure using an initial pool containing 5×10^{14} variants of 72 nt RNA with 40 nt random sequences. The selection was performed against recombinant extracellular domains of hFlt-1 fused to human IgG and a hexahistidine tag. To resist ribonuclease degradation, 2′-fluoropyrimidine modifications were introduced into the pool of RNAs.[27] To avoid enrichment of aptamers against the resins, three different resins were alternatively employed: anti-IgG aptamer-immobilized,[23] nickel-charged, and protein A-immobilized resins. To select tightly binding aptamers, we progressively increased the selection stringency by increasing the number of washings and by decreasing the target concentration for positive selection (Table 1).

After four rounds of SELEX, moderate enrichment of the pool affinity against the target was observed by the SPR analysis, and the affinity progressively increased until nine rounds had been performed (data not shown). Because further rounds of SELEX clearly enriched molecules with affinity for human IgG used as a tag protein (data not shown), clones from the pools after five to nine rounds were analyzed. Among ~200 clones randomly picked out, ~60 independent sequences were isolated. Of these, ~40 isolates showed affinity for hFlt-1, not IgG, upon SPR analysis. Thus, their inhibitory activities were

dx.doi.org/10.1021/bi301669p | Biochemistry 2013, 52, 2274−2279

examined by the VEGF-induced autophosphorylation assay for hFlt-1 using NIH 3T3 cells that ectopically express hFlt-1 (3T3-FLT-1 cells).[25] As judged from band intensities of phosphorylated hFlt-1 on Western blotting, three isolates with similar sequences, #38, #77, and #115, exhibited inhibitory activity (Figure 1A and Table 2). The hFlt-1 specificity of these

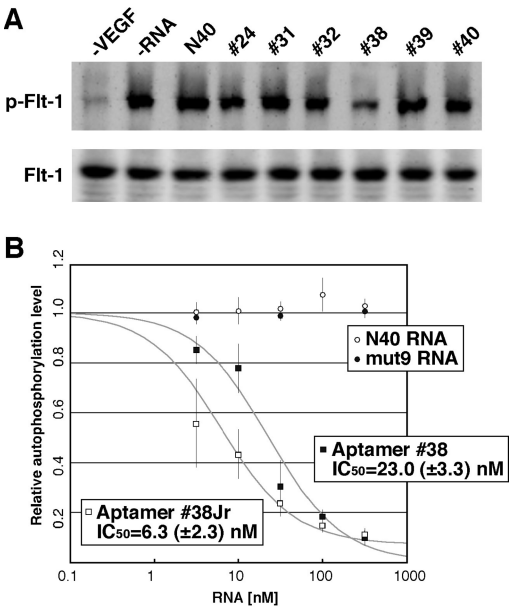

Figure 1. Inhibitory activities of the aptamers on VEGF-stimulated hFlt-1 autophosphorylation. (A) Screening of the inhibitory aptamers against hFlt-1 by Western blotting. 3T3-FLT-1 cells were incubated with the indicated aptamer RNAs (100 nM) for 5 min, and the stimulation was performed with 10 ng/mL $VEGF_{165}$ for 6 min. The top and bottom images show the detection of phosphorylated hFlt-1 (p-Flt-1) and total hFlt-1, respectively. At least two independent experiments were performed for each isolate. Lanes indicated by "−VEGF" and "−RNA" show the cells before the stimulation and the cells stimulated without the addition of RNA, respectively. (B) Quantitative analysis of the inhibitory activity by the sandwich ELISA. 3T3-FLT-1 cells were incubated with the indicated concentrations of the aptamer RNAs for 5 min, and the stimulation was performed with 10 ng/mL $VEGF_{165}$ for 6 min. Three independent duplicate experiments were conducted. The IC_{50} value was estimated by curve fitting using Gnuplot version 4.5.0 (http://www.gnuplot.info/).

Table 2. Primary Sequences of Inhibitory RNA Aptamers against hFlt-1

clone[a]	sequence (5′ to 3′)[b]
#38 (five times)	GGGCUGAAGG AU**GCCA**UA**GA GUGUUAUGUA GUGGAGGAGG AGACACAAUG GU**GGUCCCGA GUCGUGCCAU CU
#77 (four times)	GGGCUGAAGG AUGCCAUAGA GUGUUAUGUA GUGGAGGAGG AGgCACAAUG GUGGUCCCGA GUCGUGCCAU CU
#115 (once)	GGGCUGAAGG AUGCCAUgGA GUGUUAUGUA GUGGAGGAGG AGACACAgUG GUGGUCCCGA GUCGUGCCAU CU

[a]In parentheses are given the frequencies with which the sequence was selected. [b]The primer-binding sites are indicated by underlines. In the #38 sequence, the region covering the shortened aptamer (#38Jr) is highlighted in bold. In the #77 and # 115 sequences, the nucleotides different from those of clone #38 are shown with lowercase letters.

aptamers was confirmed by the SPR analysis, in which the homologous receptor, human KDR (VEGFR2), exhibited no binding signal even with 1 μM KDR (data not shown). Moreover, these aptamers did not affect the VEGF-induced autophosphorylation of human KDR in the KDR-expressing cells [KDR-3T3 cells (see below)].[26]

Of these three inhibitory aptamers, the most abundant clone, #38, was subjected to further analysis. In the sandwich ELISA, #38 showed a 50% inhibitory concentration (IC_{50}) of 23.0 ± 3.3 nM against hFlt-1 (Figure 1B). In contrast, negative control RNAs, the initial pool RNA and mut9 RNA (see below), showed no apparent inhibition (Figure 1B). Because no dissociation of hFlt-1 from the aptamer-immobilized flow cell even after a dissociation time of 30 min during SPR analysis, we could not evaluate the dissociation constants (see below). Aptamer #38 also showed the inhibitory activity on the hFlt-1 autophosphorylation assay using another cell line, human angioma cells that ectopically express hFlt-1 (AG1-G1-Flt1 cells), indicating that the inhibitory activity is not restricted on certain cell lines (Figure S1 of the Supporting Information).

Mutation Analysis of Aptamer #38. Several deletion derivatives were generated from aptamer #38 with 72 nt, and their inhibitory activity was examined. Thus, the shortened derivative, #38Jr with 40 nt, was defined to be fully active to block the Flt-1 activation (Table 2 and Figure 2). The IC_{50}

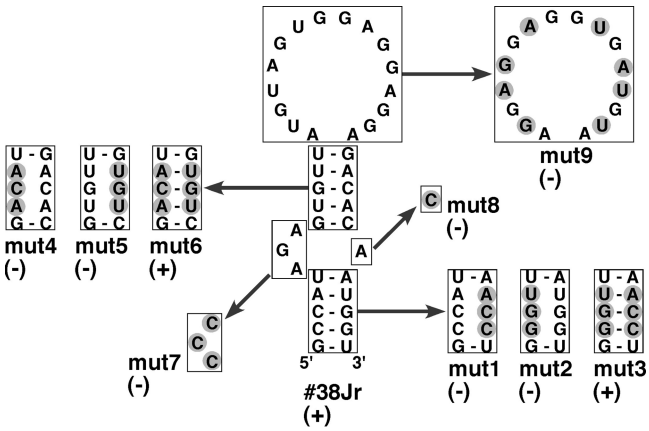

Figure 2. Mutational analysis of aptamer #38Jr. The two-dimensional structure of aptamer #38Jr is shown at the center. The mutated bases are shown with a gray background. The inhibitory activities were analyzed by Western blotting as described in the legend of Figure 1A. Two independent duplicate experiments were performed. All the mutants showed either activity comparable to that of aptamer #38Jr (indicated by a plus sign in parentheses) or undetectable activity (indicated by a minus sign).

value of #38Jr was 6.3 ± 2.3 nM as monitored by the sandwich ELISA (Figure 1B). The higher inhibitory activity of the shortened aptamer might be explained by assuming the lower frequency of alternative, inactive folding and/or elimination of some steric hindrance. As was the case for aptamer #38, aptamer #38Jr also inhibited the VEGF-stimulated hFlt-1 autophosphorylation on AG1-G1-Flt1 cells (Figure S1 of the Supporting Information).

According to the structure prediction by an energy minimization program (Mfold),[28] #38Jr was expected to adopt the secondary (2D) structure containing the terminal stem, internal loop, internal stem, and large terminal loop (Figure 2). To confirm the predicted structure, we examined the activity of base replacement derivatives of #38Jr (Figure 2). When mutations were introduced to disrupt base pairings of

dx.doi.org/10.1021/bi301669p | Biochemistry 2013, 52, 2274−2279

the terminal stem (mut1 and mut2), the activity was markedly reduced. However, the activity was completely restored by compensatory changes in the same stem (mut3). Similar results were obtained for mutations at the internal stem (mut4, mut5, and mut6). Thus, the secondary structure, not the primary sequence, of the stems is important. When single-stranded regions in the loops were mutated (mut7, mut8, and mut9), the activity was significantly reduced (Figure 2), suggesting that, like many other aptamers,[22,29−32] the primary sequences of these single-stranded regions are crucial for activity.

Elucidation of the Inhibitory Mechanism. Flt-1 requires binding of heparin to function,[33,34] and several inhibitory aptamers have been reported to interact with a heparin-binding site on a target protein.[35−38] Therefore, one might speculate that aptamer #38 binds to the heparin-binding site of hFlt-1 and competitively inhibits the association of heparin with hFlt-1. This possibility was first investigated by the pull-down experiment with heparin-immobilized resin (Figure 3). In the absence of RNA, ~10% of input hFlt-1 was recovered with the heparin resin. Under this condition, the hFlt-1 recovery was slightly reduced in the presence of 50 nM control RNA and further reduced in the presence of 500 nM control RNA, suggesting a small but significant nonspecific affinity of hFlt-1 for RNA. In contrast, aptamer #38 did not interfere with hFlt-1 recovery with the heparin resin even at high nanomolar concentrations up to 500 nM (Figure 3). Interestingly, several noninhibitory aptamers showed reduction of the hFlt-1 recovery (Figure 3). These results suggest that the inhibitory mechanism of aptamer #38 is not to hinder association of heparin with hFlt-1.

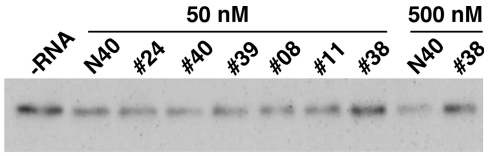

Figure 3. Effect of the aptamers on the interaction between Flt-1 and heparin. Recombinant hFlt-1 was incubated with the indicated concentrations of RNAs and then applied to heparin-immobilized resin. The hFlt-1 bound to the resin was analyzed by Western blotting. Similar results were reproducibly obtained by four independent experiments.

Next, we examined whether aptamer #38 blocks the binding of VEGF to hFlt-1 in the SPR assay. As shown in Figure 4, hFlt-1 bound to the aptamer #38-immobilized sensor chip while VEGF did not, and no appreciable release of hFlt-1 from the chip was observed during the prolonged dissociation time. When the mixture of hFlt-1 and VEGF was injected onto the sensor chip, the SPR signal was reproducibly stronger than that of hFlt-1 alone (Figure 4). These findings clearly indicate the formation of the ternary complex among aptamer #38, hFlt-1, and VEGF. It is noteworthy that the hFlt-1·VEGF complex, or VEGF, bound to the aptamer #38-immobilized sensor chip exhibits a slight dissociation unlike that of hFlt-1 alone.

No inhibitory action of aptamer #38 with respect to formation of the binary complex between hFlt-1 and VEGF was confirmed by monitoring the decoy activity of hFlt-1 in the presence of aptamer #38 (Figure 5). Because soluble Flt-1 is known to titrate VEGF, recombinant hFlt-1 inhibits the VEGF-stimulated KDR autophosphorylation of KDR-3T3 cells expressing KDR on the cell surface (Figure 5). If the aptamer could affect the association of VEGF with hFlt-1 to some extent, high concentrations of #38 might reduce the decoy activity of hFlt-1 for titration of VEGF. However, aptamer #38 did not reverse the KDR autophosphorylation even at a concentration of up to 1 μM (Figure 5). These findings again

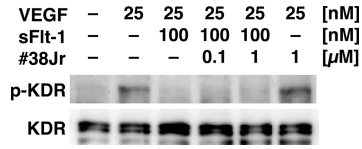

Figure 5. Effect of aptamer #38 on the decoy activity of Flt-1. The indicated concentrations of recombinant hFlt-1 and folded aptamer #38 were mixed in 100 μL of buffer A and incubated at 37 °C for 5 min. Then, 100 μL of 10 ng/mL $VEGF_{165}$ dissolved in buffer A was added to the mixture and applied to 3T3-KDR cells. The stimulation was performed for 6 min and analyzed by Western blotting. Phosphorylated (p-KDR) and total KDR were detected with anti-phospho-tyrosine and anti-KDR antibodies (top and bottom panels, respectively). The reproducibility was confirmed by three independent duplicate experiments.

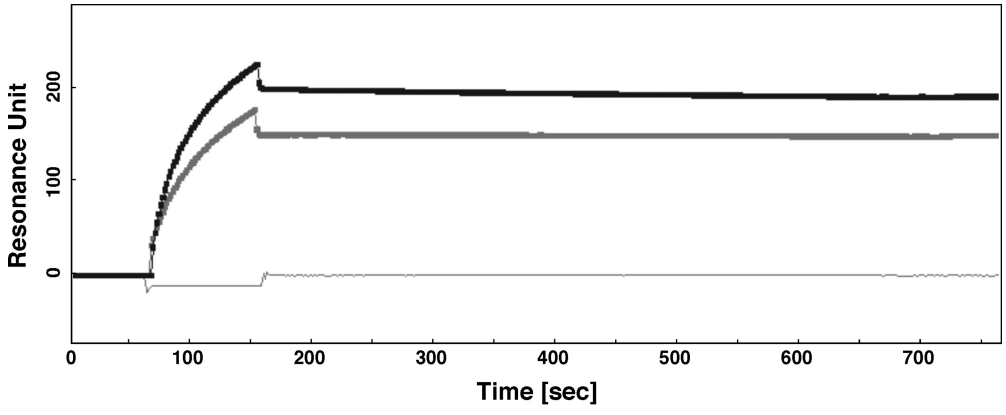

Figure 4. SPR analysis of the formation of the ternary complex of aptamer #38, hFlt-1, and VEGF. SPR analysis was performed by using the aptamer #38-immobilized sensor chip. Lines marked by gray and black squares show sensorgrams of 100 ng/mL recombinant hFlt-1 alone and a mixture of 25 ng/mL $VEGF_{165}$ and 100 ng/mL recombinant hFlt-1, respectively. A line without marks shows a sensorgram of 25 ng/mL $VEGF_{165}$. Similar results were reproducibly obtained by three independent experiments.

dx.doi.org/10.1021/bi301669p | *Biochemistry* 2013, 52, 2274−2279

point out that the inhibitory mechanism of aptamer #38 is not to hinder the binding of VEGF to Flt-1. A similar result was also obtained by the chemical cross-linking experiment in vitro (data not shown).

DISCUSSION

In this study, we isolated inhibitory RNA aptamers against hFlt-1. One of the original isolates, aptamer #38, with 72 nt was shortened to 40 nt without losing activity, giving rise to aptamer #38Jr. The 2D structure of aptamer #38Jr was confirmed by mutational analysis, and the importance of primary sequences of the loop regions, not the stems, was revealed (Figure 3). Because half of the residues in the terminal loop (8 of 16) are guanines, the loop may adopt a guanine quadruplex conformation, one of the structures frequently found in small, structural RNAs, including aptamers.[39] In our preliminary analysis, aptamer #38Jr showed the typical circular dichroism spectra of the antiparallel guanine quadruplex structure (data not shown).

Aptamer #38 possesses interesting features. First, aptamer #38 does not interfere with the association of hFlt-1 with heparin, whereas several noninhibitory aptamers do (Figure 3). This might explain why only three of ~40 aptamers (or only 10 of ~200 clones sequenced) showed inhibitory activity. Similar to RNA, heparin is a negatively charged polymer with glycol moieties, and heparin-binding sites are frequently targeted by aptamers.[35−38] Flt-1 harbors a heparin-binding site, and the heparin binding to Flt-1 is necessary for VEGF-mediated activation of Flt-1. However, aptamer #38 does not interfere with binding of heparin to hFlt-1, indicating that the inhibitory mechanism is not to compete with heparin.

Second, aptamer #38 does not inhibit the binding of VEGF to hFlt-1 when examined by SPR analysis using the aptamer #38-immobilized sensor chip (see Figure 4) as well as by the cell-based decoy assay of hFlt-1 to block VEGF-induced autophosphorylation of KDR (see Figure 5). Therefore, aptamer #38 may block the conformational change necessary for autophosphorylation of hFlt-1 regardless of whether it is bound to VEGF. Although the exact inhibitory mechanism remains to be investigated, aptamer #38 provides us with a unique tool to inhibit Flt-1 alone, unlike the other known anti-Flt-1 inhibitors. For example, anti-Flt-1 antibodies affect not only Flt-1-mediated signaling but also KDR-mediated signaling through dysfunction of the decoy activity of Flt-1. Therefore, aptamer #38 will prove to be useful in achieving the blockade of Flt-1-mediated signaling without affecting the decoy function of Flt-1 to avoid undesired side effects that lead to the promotion of angiogenesis.

ASSOCIATED CONTENT

Supporting Information

Supporting figure (Figure S1). This material is available free of charge via the Internet at http://pubs.acs.org.

AUTHOR INFORMATION

Corresponding Author

*Telephone: 81(JPN)-3-5449-5307. Fax: 81(JPN)-3-5449-5415. E-mail: nak@ims.u-tokyo.ac.jp.

Funding

This work was funded by a Core Research for Evolution Science and Technology (CREST) grant from the Japan Science and Technology Agency (to Y.N.), research grants from The Ministry of Education, Sports, Culture, Science and Technology of Japan (MEXT) (to Y.N.) and The Ministry of Health, Labour and Welfare (to Y.N.), and a Grant-in-aid Special Project Research on Cancer-Bioscience 17014020 from MEXT (to M.S.).

Notes

The authors declare no competing financial interest.

ACKNOWLEDGMENTS

We thank Akiko Oide and Kayo Kobayashi for technical assistance and Drs. Shin Miyakawa and Satoko Yamazaki for providing the anti-IgG aptamer-immobilized resin. We also thank Drs. Sachiko Yamaguchi and Mai Yamauchi for technical advice with the autophosphorylation assays.

ABBREVIATIONS

VEGF, vesicular endothelial growth factor; VEGFR, VEGF receptor; PlGF, placental growth factor; hFlt-1, human Flt-1; SELEX, systematic evolution of ligands by exponential enrichment.

REFERENCES

(1) Lohela, M., Bry, M., Tammela, T., and Alitalo, K. (2009) VEGFs and receptors involved in angiogenesis versus lymphangiogenesis. *Curr. Opin. Cell Biol. 21*, 154−165.

(2) Takahashi, H., and Shibuya, M. (2005) The vascular endothelial growth factor (VEGF)/VEGF receptor system and its role under physiological and pathological conditions. *Clin. Sci. 109*, 227−241.

(3) Shibuya, M., and Claesson-Welsh, L. (2006) Signal transduction by VEGF receptors in regulation of angiogenesis and lymphangiogenesis. *Exp. Cell Res. 312*, 549−560.

(4) Fong, G. H., Rossant, J., Gertsenstein, M., and Breitman, M. L. (1995) Role of the Flt-1 receptor tyrosine kinase in regulating the assembly of vascular endothelium. *Nature 376*, 66−70.

(5) Hiratsuka, S., Minowa, O., Kuno, J., Noda, T., and Shibuya, M. (1998) Flt-1 lacking the tyrosine kinase domain is sufficient for normal development and angiogenesis in mice. *Proc. Natl. Acad. Sci. U.S.A. 95*, 9349−9354.

(6) Ferrara, N. (2001) Role of vascular endothelial growth factor in regulation of physiological angiogenesis. *Am. J. Physiol. 280*, C1358−C1366.

(7) Hattori, K., Heissig, B., Wu, Y., Dias, S., Tejada, R., Ferris, B., Hicklin, D. J., Zhu, Z., Bohlen, P., Witte, L., Hendrikx, J., Hackett, N. R., Crystal, R. G., Moore, M. A., Werb, Z., Lyden, D., and Rafii, S. (2002) Placental growth factor reconstitutes hematopoiesis by recruiting VEGFR1+ stem cells from bone-marrow microenvironment. *Nat. Med. 8*, 841−849.

(8) LeCouter, J., Moritz, D. R., Li, B., Phillips, G. L., Liang, X. H., Gerber, H. P., Hillan, K. J., and Ferrara, N. (2003) Angiogenesis-independent endothelial protection of liver: Role of VEGFR-1. *Science 299*, 890−893.

(9) Carmeliet, P., Moons, L., Luttun, A., Vincenti, V., Compernolle, V., De Mol, M., Wu, Y., Bono, F., Devy, L., Beck, H., Scholz, D., Acker, T., DiPalma, T., Dewerchin, M., Noel, A., Stalmans, I., Barra, A., Blacher, S., Vanden-driessche, T., Ponten, A., Eriksson, U., Plate, K. H., Foidart, J. M., Schaper, W., Charnock-Jones, D. S., Hicklin, D. J., Herbert, J. M., Collen, D., and Persico, M. G. (2001) Synergism between vascular endothelial growth factor and placental growth factor contributes to angiogenesis and plasma extravasation in pathological conditions. *Nat. Med. 7*, 575−583.

(10) Luttun, A., Brusselmans, K., Fukao, H., Tjwa, M., Ueshima, S., Herbert, J. M., Matsuo, O., Collen, D., Carmeliet, P., and Moons, L. (2002) Loss of placental growth factor protects mice against vascular permeability in pathological conditions. *Biochem. Biophys. Res. Commun. 295*, 428−434.

(11) Fischer, C., Mazzone, M., Jonckx, B., and Carmeliet, P. (2008) FLT1 and its ligands VEGFB and PlGF: Drug targets for anti-angiogenic therapy? *Nat. Rev. Cancer 8*, 942−956.
(12) Luttun, A., Tjwa, M., Moons, L., Wu, Y., Angelillo-Scherrer, A., Liao, F., Nagy, J. A., Hooper, A., Priller, J., De Klerck, B., Compernolle, V., Daci, E., Bohlen, P., Dewerchin, M., Herber, J. M., Fava, R., Matthys, P., Carmeliet, G., Collen, D., Dvorak, H. F., Hicklin, D. J., and Carmeliet, P. (2002) Revascularization of ischemic tissues by PlGF treatment, and inhibition of tumor angiogenesis, arthritis and atherosclerosis by anti-Flt1. *Nat. Med. 8*, 831−840.
(13) Pavco, P. A., Bouhana, K. S., Gallegos, A. M., Agrawal, A., Blanchard, K. S., Grimm, S. L., Jensen, K. L., Andrews, L. E., Wincott, F. E., Pitot, P. A., Tressler, R. J., Cushman, C., Reynolds, M. A., and Parry, T. J. (2000) Antitumor and antimetastatic activity of ribozymes targeting the messenger RNA of vascular endothelial growth factor receptors. *Clin. Cancer Res. 6*, 2094−2103.
(14) Kobayashi, H., Eckhardt, S. G., Lockridge, J. A., Rothenberg, M. L., Sandler, A. B., O'Bryant, C. L., Cooper, W., Holden, S. N., Aitchison, R. D., Usman, N., Wolin, M., and Basche, M. L. (2005) Safety and pharmacokinetic study of RPI.4610 (ANGIOZYME), an anti-VEGFR-1 ribozyme, in combination with carboplatin and paclitaxel in patients with advanced solid tumors. *Cancer Chemother. Pharmacol. 56*, 329−336.
(15) Weng, D. E., Masci, P. A., Radka, S. F., Jackson, T. E., Weiss, P. A., Ganapathi, R., Elson, P. J., Capra, W. B., Parker, V. P., Lockridge, J. A., Cowens, J. W., Usman, N., and Borden, E. C. (2005) A phase I clinical trial of a ribozyme-based angiogenesis inhibitor targeting vascular endothelial growth factor receptor-1 for patients with refractory solid tumors. *Mol. Cancer Ther. 4*, 948−955.
(16) Shen, J., Samul, R., Silva, R. L., Akiyama, H., Liu, H., Saishin, Y., Hackett, S. F., Zinnen, S., Kossen, K., Fosnaugh, K., Vargeese, C., Gomez, A., Bouhana, K., Aitchison, R., Pavco, P., and Campochiaro, P. A. (2006) Suppression of ocular neovascularization with siRNA targeting VEGF receptor 1. *Gene Ther. 13*, 225−234.
(17) Kleinman, M. E., Yamada, K., Takeda, A., Chandrasekaran, V., Nozaki, M., Baffi, J. Z., Albuquerque, R. J., Yamasaki, S., Itaya, M., Pan, Y., Appukuttan, B., Gibbs, D., Yang, Z., Karikó, K., Ambati, B. K., Wilgus, T. A., DiPietro, L. A., Sakurai, E., Zhang, K., Smith, J. R., Taylor, E. W., and Ambati, J. (2008) Sequence- and target-independent angiogenesis suppression by siRNA via TLR3. *Nature 452*, 591−597.
(18) Joyce, G. F. (2007) Forty years of in vitro evolution. *Angew. Chem., Int. Ed. 46*, 6420−6436.
(19) Ellington, A., and Szostak, J. W. (1990) *In vitro* selection of RNA molecules that bind specific ligands. *Nature 346*, 818−822.
(20) Tuerk, C., and Gold, L. (1990) Systematic evolution of ligands by exponential enrichment: RNA ligands to bacteriophage T4 DNA polymerase. *Science 249*, 505−510.
(21) Klussmann, S. (2006) *The Aptamer Handbook: Functional Oligonucleotides and Their Applications*, Wiley-VCH, Weinheim, Germany.
(22) Ohuchi, S. P., Ohtsu, T., and Nakamura, Y. (2006) Selection of RNA aptamers against recombinant transforming growth factor-β type III receptor displayed on cell surface. *Biochimie 88*, 897−904.
(23) Miyakawa, S., Nomura, Y., Sakamoto, T., Yamaguchi, Y., Kato, K., Yamazaki, S., and Nakamura, Y. (2008) Structural and molecular basis for hyperspecificity of RNA aptamer to human immunoglobulin G. *RNA 14*, 1154−1163.
(24) Iwagawa, T., Ohuchi, S. P., Watanabe, S., and Nakamura, Y. (2012) Selection of RNA aptamers against mouse embryonic stem cells. *Biochimie 94*, 250−257.
(25) Kobayashi, S., Sawano, A., Nojima, Y., Shibuya, M., and Maru, Y. (2004) The c-Cbl/CD2AP complex regulates VEGF-induced endocytosis and degradation of Flt-1 (VEGFR-1). *FASEB J. 18*, 929−931.
(26) Takahashi, T., and Shibuya, M. (1997) The 230 kDa mature form of KDR/Flk-1 (VEGF receptor-2) activates the PLC-γ pathway and partially induces mitotic signals in NIH3T3 fibroblasts. *Oncogene 14*, 2079−2089.
(27) Pieken, W., Olsen, D., Benseler, F., Aurup, H., and Eckstein, F. (1991) Kinetic characterization of ribonuclease-resistant 2′-modified hammerhead ribozymes. *Science 253*, 314−317.
(28) Zuker, M. (2003) Mfold web server for nucleic acid folding and hybridization prediction. *Nucleic Acids Res. 31*, 3406−3415.
(29) Zhai, G., Iskandar, M., Barilla, K., and Romaniuk, P. (2001) Characterization of RNA aptamer binding by the Wilms' tumor suppressor protein WT1. *Biochemistry 40*, 2032−2040.
(30) Boese, B., and Breaker, R. (2007) *In vitro* selection and characterization of cellulose-binding DNA aptamers. *Nucleic Acids Res. 35*, 6378−6388.
(31) Skrisovska, L., Bourgeois, C., Stefl, R., Grellscheid, S., Kister, L., Wenter, P., Elliott, D., Stevenin, J., and Allain, F. (2007) The testis-specific human protein RBMY recognizes RNA through a novel mode of interaction. *EMBO Rep. 8*, 372−379.
(32) Goers, E., Voelker, R., Gates, D., and Berglund, J. (2008) RNA binding specificity of Drosophila muscleblind. *Biochemistry 47*, 7284−7294.
(33) Ito, N., and Claesson-Welsh, L. (1999) Dual effects of heparin on VEGF binding to VEGF receptor-1 and transduction of biological responses. *Angiogenesis 3*, 159−166.
(34) Park, M., and Lee, S. T. (1999) The fourth immunoglobulin-like loop in the extracellular domain of FLT-1, a VEGF receptor, includes a major heparin-binding site. *Biochem. Biophys. Res. Commun. 264*, 730−734.
(35) Lee, J. H., Canny, M. D., De Erkenez, A., Krilleke, D., Ng, Y. S., Shima, D. T., Pardi, A., and Jucker, F. (2005) A therapeutic aptamer inhibits angiogenesis by specifically targeting the heparin binding domain of VEGF165. *Proc. Natl. Acad. Sci. U.S.A. 102*, 18902−18907.
(36) Jeter, M. L., Ly, L. V., Fortenberry, Y. M., Whinna, H. C., White, R. R., Rusconi, C. P., Sullenger, B. A., and Church, F. C. (2004) RNA aptamer to thrombin binds anion-binding exosite-2 and alters protease inhibition by heparin-binding serpins. *FEBS Lett. 568*, 10−14.
(37) Marro, M. L., Daniels, D. A., Andrew, D. P., Chapman, T. D., and Gearing, K. L. (2006) *In vitro* selection of RNA aptamers that block CCL1 chemokine function. *Biochem. Biophys. Res. Commun. 349*, 270−276.
(38) Long, S. B., Long, M. B., White, R. R., and Sullenger, B. A. (2008) Crystal structure of an RNA aptamer bound to thrombin. *RNA 14*, 2504−2512.
(39) Ji, X., Sun, H., Zhou, H., Xiang, J., Tang, Y., and Zhao, C. (2011) Research progress of RNA quadruplex. *Nucleic Acid Ther. 21*, 185−200.